U.S. ARMY

U.S. ARMY COMBAT CAPABILITIES DEVELOPMENT COMMAND
CHEMICAL BIOLOGICAL CENTER
ABERDEEN PROVING GROUND, MD 21010-5424

DEVCOM CBC-TR-1888

Design and Application of an Adept Aerosol Lung-on-a-Chip and Aerosol and Vapor Delivery Systems

Dylan H. Fudge
Priscilla Lee
Ronald Evans
Tyler D. P. Goralski
RESEARCH AND OPERATIONS DIRECTORATE

Bradley Ruprecht
ENGINEERING DIRECTORATE

June 2024

Disclaimer

The findings in this report are not to be construed as an official Department of the Army position unless so designated by other authorizing documents.

REPORT DOCUMENTATION PAGE

1. REPORT DATE	2. REPORT TYPE	3. DATES COVERED	
		START DATE	END DATE
XX-06-2024	Final	Sep 2021	Sep 2022

4. TITLE AND SUBTITLE
Design and Application of an Adept Aerosol Lung-on-a-Chip and Aerosol and Vapor Delivery Systems

5a. CONTRACT NUMBER	5b. GRANT NUMBER	5c. PROGRAM ELEMENT NUMBER
5d. PROJECT NUMBER	**5e. TASK NUMBER**	**5f. WORK UNIT NUMBER**

6. AUTHOR(S)
Fudge, Dylan H.; Lee, Priscilla; Evans, Ronald; Goralski, Tyler D. P.; Ruprecht, Bradley

7. PERFORMING ORGANIZATION NAME(S) AND ADDRESS(ES)	8. PERFORMING ORGANIZATION REPORT NUMBER
Director, DEVCOM CBC, ATTN: FCDD-CBR-TM, APG, MD 21010-5424	DEVCOM CBC-TR-1888

9. SPONSORING/MONITORING AGENCY NAME(S) AND ADDRESS(ES)	10. SPONSOR/MONITOR'S ACRONYM(S)	11. SPONSOR/MONITOR'S REPORT NUMBER(S)
U.S. Army Combat Capabilities Development Command Chemical Biological Center; 5183 Blackhawk Road; Aberdeen Proving Ground, MD 21010-5424	DEVCOM CBC	

12. DISTRIBUTION/AVAILABILITY STATEMENT
Distribution Statement A. Approved for public release: distribution is unlimited.

13. SUPPLEMENTARY NOTES
This work was funded by DoD Funding Laboratory Enhancements Across Four Categories (FLEX-4), Section 2363.

14. ABSTRACT (LESS THAN 200 WORDS)
Organ-on-a-chip technology and other microphysiological systems were designed to recreate living tissues that mimic organ microenvironments through precise control of the cells, extracellular matrix, and other microenvironmental factors. While correcting many of the gaps present in traditional tissue culture with a more physiologically relevant model, these systems still suffer from limitations. The inability to accurately administer aerosols and vapors to the lung epithelial cells is a specific limitation to current lung-on-a-chip technology. Having the capability to perform testing and analysis on tissues through conventional routes of exposure specific to the organ is paramount in achieving a complete biologically relevant system. To close this gap, we combined 3D printing technology with microfluidic organ chip engineering to build a customizable open-top lung chip specific for the evaluation of aerosol and vapor toxicity and efficacy testing. 3D printing technology was additionally used to design an aerosol and vapor delivery chamber specific to the open-top lung chips. This approach overall allowed for customizable time- and cost-effective parts to efficiently optimize a novel aerosol and vapor delivery system for lung tissue exposures. Overall, in this study, we designed, generated, and evaluated novel open-top lung chip designs that will be used to expand our capabilities.

15. SUBJECT TERMS

Organ-on-a-chip (OOC)	Aerobiology	Aerosol
Microphysiological system (MPS)	Toxicology	Vapor
Additive manufacturing	3D printing	

16. SECURITY CLASSIFICATION OF:			17. LIMITATION OF ABSTRACT	18. NUMBER OF PAGES
a. REPORT	b. ABSTRACT	C. THIS PAGE		
U	U	U	UU	38

19a. NAME OF RESPONSIBLE PERSON	19b. PHONE NUMBER *(Include area code)*
Renu B. Rastogi	(410) 436-7545

STANDARD FORM 298 (REV. 5/2020)
Prescribed by ANSI Std. Z39.18

Blank

PREFACE

The work described in this report was authorized under DoD Funding Laboratory Enhancements Across Four Categories (FLEX-4), Section 2363 for fiscal years 2021 and 2022. The work was started in September 2021 and completed in September 2022.

The use of either trade or manufacturers' names in this report does not constitute an official endorsement of any commercial products. This report may not be cited for purposes of advertisement.

U.S. Army Combat Capabilities Development Command Chemical Biological Center (DEVCOM CBC; Aberdeen Proving Ground, MD) was previously known as U.S. Army Edgewood Chemical Biological Center (ECBC).

This report has been approved for public release.

Blank

CONTENTS

FIGURES

TABLES

DESIGN AND APPLICATION OF AN ADEPT AEROSOL LUNG-ON-A-CHIP AND AEROSOL AND VAPOR DELIVERY SYSTEMS

1. INTRODUCTION

Despite the enormous progress made using traditional cell cultures and animal models, more advanced tools are required to answer the complex questions veiling current biological research. Conventional models such as 2D monolayers or 3D extracellular matrixes and spheroids provide a biologically controllable environment for scientific analysis. However, conventional methods lack the 3D cellular complexity and organization present in physiological tissue. In addition, conventional models lack mimicry of organ-specific physiological microenvironments such as mechanical forces and chemical gradients. Although animal models accomplish these tasks, they often do not match human responses, and their use can raise major economic and ethical concerns. Progress in microengineering technology offers a solution by providing an option that overcomes many of the drawbacks associated with traditional tissue culture and animal modeling: cutting-edge microphysiological systems (MPSs) that imitate human tissue–tissue interfaces, the chemical and mechanical microenvironments that are specific to living human organs. These microphysiological systems are collectively known as organs-on-a-chip (OOCs). From the combined research efforts of microfluidic and tissue engineering, OOCs answer the need for biologically relevant human organ model systems. These biomimetic MPSs aim to recreate the tissue organization and physical forces exerted on cells in specific organs, thereby offering a complementary or superior alternative to animal or conventional cell culture models for the study of infectious disease.

One of the major advantages OOC systems offer is the introduction of mechanical stimuli to the model. These include fluid shear force, concentration gradient, dynamic mechanical stress, and cell patterning. The mechanical forces present due to microfluidics in OOCs have proven paramount in providing a physiologically sound representation of human organs. For example, the cells within the gut will reorganize into 3D villi structures only when exposed to shear stress; and kidney cells will reorganize their cytoskeleton, leading to the expression of differentiated epithelial cell functions. In addition to mechanical stimuli, OOCs can also introduce optical and electrical stimuli, for example, in cardiac tissue.

OOCs and other MPSs were designed to recreate living tissues or organ microenvironments through precise control of the cells, extracellular matrix, and other microenvironmental factors to investigate physiological or pathological mechanisms. However, these systems still have limitations. The inability to administer aerosols to the lung epithelial cells is a specific limitation of the lung chips. Having the capability to perform testing and analysis on tissues through conventional routes of exposure specific to the organ is paramount in achieving a biologically relevant system. Many mechanisms exist for creating aerosols and vapors; however, a true commercially available aerosol delivery system has not been successfully executed in OOCs or other MPSs. By producing an aerosol and vapor delivery system amenable to a lung chip, we will fill this gap in our current technology, thereby enhancing and expanding the testing repertoire available for lung microenvironments. This requires the development of a novel open-top lung chip design with an adaptable aerosol and

vapor system that seamlessly interfaces with the lung chip platforms (Figure 1). The manufacturing process for developing the novel open-top lung chip design and the paired aerosol and vapor delivery system will take advantage of the Boston Micro Fabrication (BMF; Maynard, MA) 3D printing facilities at the U.S. Army Combat Capabilities Development Command Chemical Biological Center (DEVCOM CBC; Aberdeen Proving Ground, MD).

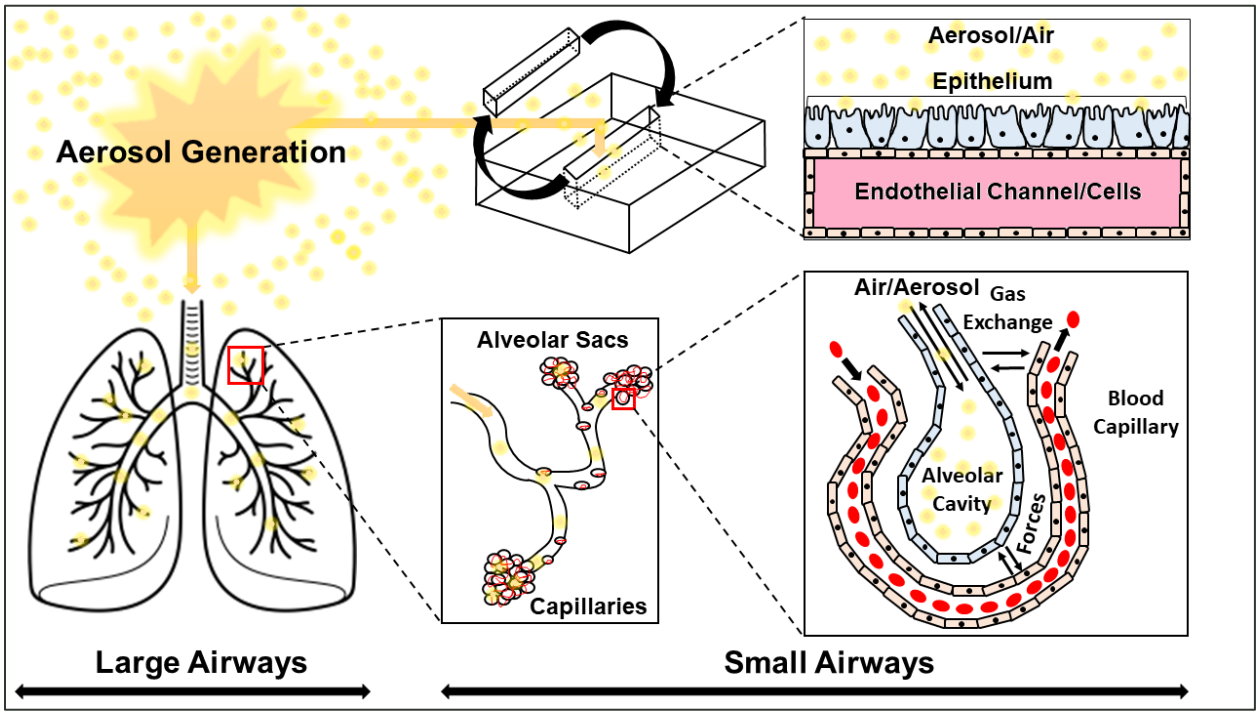

Figure 1. Objective to deposit aerosol on lung-on-a-chip.

Novel chip design, such as that developed at Emulate (formerly Wyss Institute; Boston, MA), requires photoetching to construct the molds for casting chip components. Photoetching is predominantly chosen for manufacturing high-resolution, low-micron structures. Although the photoetching manufacturing process works well, it is cumbersome and costly. It requires highly specialized equipment, a clean room, and multiple complex fabrication steps, which translate to long lead times and high costs for chip manufacturing.

We plan to use modern 3D printing as a more cost-effective and updated manufacturing process for organ chip fabrication without sacrificing product quality. Stereolithography (SLA) is the primary method used for 3D printing. Current SLA hardware at DEVCOM CBC has a 60 µm feature-resolution limit. This will suffice for two of the three required master molds. However, the membrane master mold incorporates features that are between 5 and 7 µm. Microscale SLA is used to eliminate the photoetching process while still permitting the necessary low-micron features in the membrane master mold. Building this final low-micron master mold requires collaboration with BMF personnel. The membrane master mold will be manufactured at the micro scale with a feature-resolution limit of 2 µm. Once the master molds are complete, chip components will be cast using the 3D-printed master molds and

injection molded using polydimethylsiloxane (PDMS) as the biocompatible material for the chips. Each PDMS layer will then be stacked and fused into a finished organ chip. 3D printing technologies greatly simplify the traditional photolithography processes, reducing the need for experimental procedures and dramatically reducing processing costs and time. Integration between organ chip engineering and 3D printing in the manufacturing process provides new opportunities for building more physiologically relevant organ chips in a more timely and cost-effective manner.

In addition to using 3D-printing technology to design novel lung chips, we take advantage of this technology to design an aerosol and vapor delivery chamber specific to the lung chips. The ease that 3D printing provides for customizable and cost-effective parts allows us to apply this technology to manufacture novel aerosol and vapor delivery systems and adapt these systems to expose human tissues in vitro. DEVCOM CBC has a long history of work in aerosol and vapor generation.

Aerosols are a liquid, solid, or both suspended in a carrier gas. Aerosols are often complex mixtures of many different compounds in multiple physical states (solid, liquid, and gas) undergoing constant changes due to chemical equilibria and physical forces. Understanding aerosols involves many different disciplines including chemistry, physics, and engineering. The manipulation and characterization of an aerosol profile is complicated when considering environmental factors that impact the aerosol, such as human respiration. Environmental factors include humidity, respiration rates, temperature, etc. Many physical factors must be considered when designing an aerosol system that will deposit physiologically relevant aerosols on alveolar cells in vitro.

The intended target for the aerosols is the deep lung or pulmonary region (alveolar ducts and alveoli), as shown in Figure 1. To reach the pulmonary region of the lungs, aerosol particles are typically <3 μm, and they deposit via sedimentation or diffusion (Brownian motion; Figure 2). The aerosol generation system used was optimized to produce particles with a mean median aerodynamic diameter (MMAD) of ~1.5 μm, which falls within the range of respirable aerosol particle sizes for the pulmonary region of the lungs. Vapors are aerosol components that consist of a compound in the gaseous physical state. However, depending on the compound, vapors may be the major component of a chemical threat.

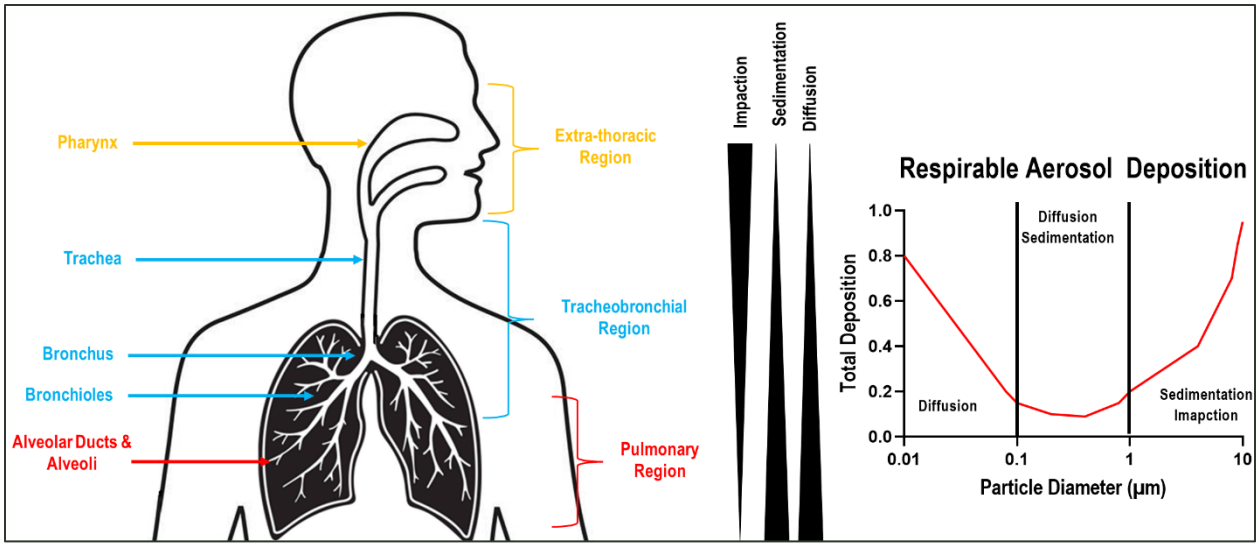

Figure 2. Respirable aerosol profile and target lung region. Many of the factors shown are simplified, such as the compound being in a homogenous solution and simply existing in a vapor phase. Controlling the degree of vaporization depends on the vapor pressure of the compound, temperature, and pressure.

The mechanism used for aerosol generation was a double-needle atomizer (DNA; patent number US 9,016,671 B1).[1] In this system, an inner needle extrudes the intended liquid to be aerosolized and the outer needle releases pressurized gas (compressed air). The inner needle (with the liquid solution) extends beyond the outer needle tip. When the liquid forms at the inner needle tip, it is dispersed by the pressurized air. This disrupts the intermolecular forces (van der Waals forces and dipole–dipole interactions) that sustain the compound as one cohesive liquid.

2. METHODS

2.1 Materials and Equipment

Materials used in this work included the following:

- 200 proof ethanol (solvent used for aerosol);
- methacholine chloride;
- Somos WaterShed XC 11122 resin (Stratasys; Eden Prairie, MN);
- Somos 9120 resin (Stratasys);
- ethanol, high-performance liquid chromatography (HPLC) grade or higher (Sigma-Aldrich; St. Louis, MO);
- methanol, HPLC grade or higher (Sigma-Aldrich);
- acetonitrile, HPLC grade or higher (Sigma-Aldrich); and
- 18 MΩ deionized water.

Tools and equipment used in this work included the following:

- DNA aerosol generator;
- DustTrak optical aerosol monitor (TSI; Shoreview, MN) and Grimm particle counter (Durag Group; Hamburg, Germany) monitoring equipment
- personal protective equipment: M-40 mask, surgical and nitrile gloves, chemically resistant boots and shoes, laboratory coat, and laboratory safety glasses;
- 5850EM series mass flow controllers (Brooks Instrument; Hatfield, PA);
- carbon capsule, lot no. 011719 WVT, catalog no. 28145-702 (Pall Life Sciences; Port Washington, NY);
- air compressors, model 1531-107B-G557X (Gast Manufacturing; Benton Harbor, MI);
- high-efficiency particulate-free air (HEPA) capsule, catalog no. NC0501487 (Cytiva; Marlborough, MA);
- 1700 series gastight removable needle syringe (Hamilton Company; Reno, NV);
- G3P-12 spin coater (Specialty Coating Systems; Indianapolis, IN);
- PE-50 XL benchtop low-pressure plasma system (Plasma Etch; Carson City, NV);
- Viper SLA system (3D Systems; Rock Hill, SC);
- ProJet 7000 HD 3D printer (3D Systems);
- 1200 series liquid chromatograph coupled to a 6490 triple-quadrupole mass spectrometer (Agilent Technologies; Santa Clara, CA);
- Supor 200 membrane disc filters (Cytiva); and
- Gilibrator calibrator (Sensidyne; St. Petersburg, FL).

2.2 Nose-Cone Aerosol System

Filter systems and one cascade impactor were used for the aerosol experiments. The filter's purpose was to collect the total amount of aerosolized compound, and the cascade impactor collected the total aerosol produced but separated the aerosol particles by size. Both the filters and the cascade impactor required assembly prior to use.

The two filter systems were opened, and the metal filter screen was placed on the bottom of the filter assembly (Figure 3A). Tweezers were used to grab a Teflon filter (Supor 200, 0.2 μm) and place it on the bottom of the filter system, on top of the metal filter (Figure 3B). The top of the filter system was placed into the lower half with the metal and Teflon filters (Figure 3C). The outer fitting was turned to seal and hold the filter system in place (Figure 3D). These steps were repeated for the other filter used (total of two filters used).

Next, the cascade impactor was assembled for use. The O-ring at the bottom of the cascade impactor was removed (Figure 3E). Another Teflon filter was placed in the bottom of the cascade impactor, and an inner O-ring was placed over the Teflon filter (Figure 3F). Filter screens were placed on top of each stage (seven stages) of the cascade impactor (Figure 3G). Tweezers were used to place the filter screens onto the stages of the cascade impactor. Vacuum grease was spread over the top of each stage of the cascade impactor filter screens to catch the

dried aerosolized material (Figure 3H). The leftover vacuum grease was used to lubricate the O-ring attachments on the outside of the two filter sets and the cascade impactor. The separate stages of the cascade impactor were loaded with the bottom (stage 7) and the top (stage 1). The bottom of the cascade impactor was assembled, which completed the assembly of the cascade impactor and filter sets.

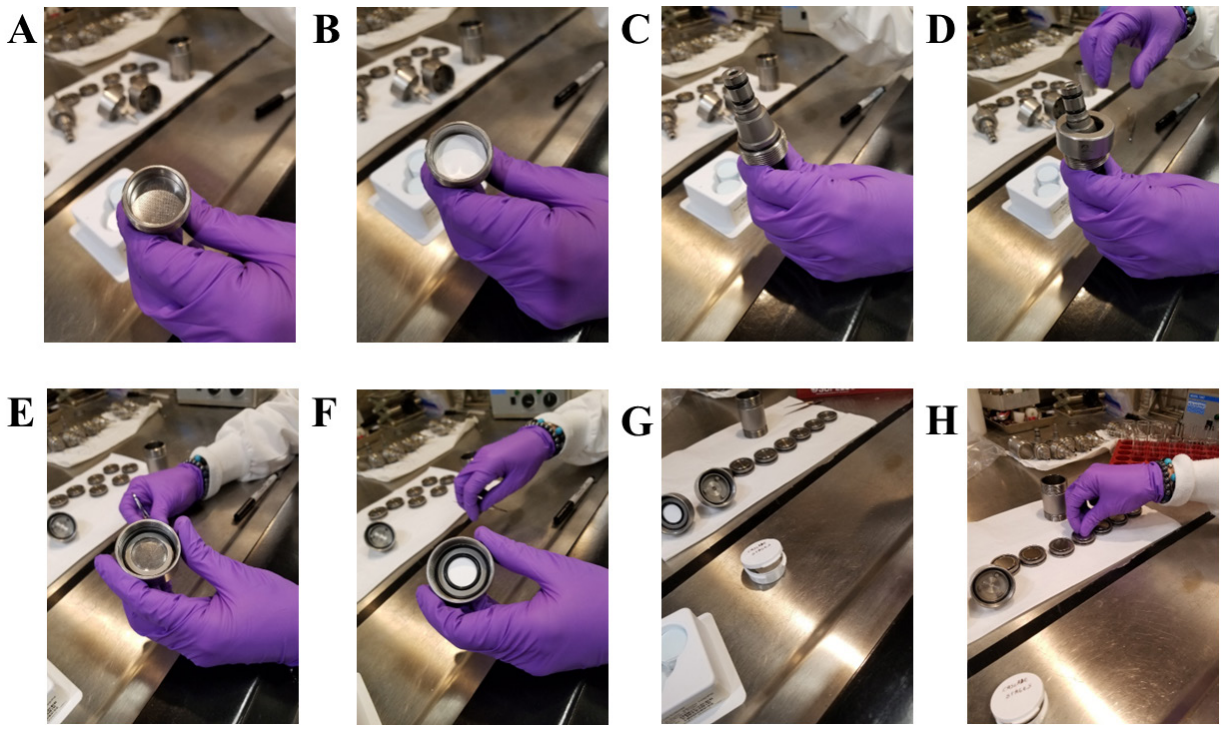

Figure 3. Filter and cascade impactor assembly for nose-cone aerosol system. (A–D) assembly of filter; (E–F) assembly of cascade impactor.

All the steps described here were performed 20 cm inside a fume hood while workers wore gloves. A Hamilton 1700 series gastight removable needle syringe was filled with a compound of interest to aerosolize using the following technique. A clean plunger and needle were attached to the syringe. The needles were always handled on flat surfaces using tweezers to avoid penetration through the workers' gloves. Approximately 250 µL of 70% ethanol was drawn up into the clean syringe. In the same manner used to assemble the clean needle, the dirty needle (used to hold the compound of interest) was assembled using plungers and needles that had come into contact with the compound of interest. Before the needle was inserted to the syringe, the white ferrule cap was removed. The compound of interest was drawn into the needle and air was removed from the syringe by drawing the solution up and down quickly. When the solution was drawn up from the storage container septum, the container was not inverted, as is common in medical practice, to avoid the solution containing the compound of interest from escaping even slightly. The solution was pulled out of the needle down into the plunger so that the needle with the previously removed white ferrule screwcap could be removed for transport to the fume hood. Throughout this process, "clean" and "dirty" zones were maintained within the fume hood to physically separate all the materials. The clean plunger was used to clean out the

remaining compound of interest within the needle using the ethanol that was drawn up earlier. The waste was dispensed into a waste container while the tip of the needle was kept below the waste container lid.

In the fume hood, the screwcap was removed to push through any air at the end of the syringe until liquid was barely seen on the white ferrule. The syringe was attached to the DNA while taking care not to bend the line leading to the DNA or twist the line when screwing the syringe to the DNA (refer to patent no. US 9,016,671 B1.[1]) The metal base of the needle was twisted to avoid cracking the glass syringe. Once the needle was loaded, it was placed into the syringe drive. The plunger wings were flush against the drive block, and the back plate was flush against the syringe plunger. A small amount of compound of interest was pushed through the DNA line to prime it (~35 µL). The correct internal diameter of the syringe was input into the syringe drive for proper drive speed. The nose-cone-only aerosol system was turned on in the following order (Figure 4):

1. syringe drive,
2. DustTrak monitor,
3. vacuum line for DNA,
4. vacuum to the hood,
5. vacuum pump,
6. compressed air cylinder and regulator (opened), and
7. mass flow controllers (always on).

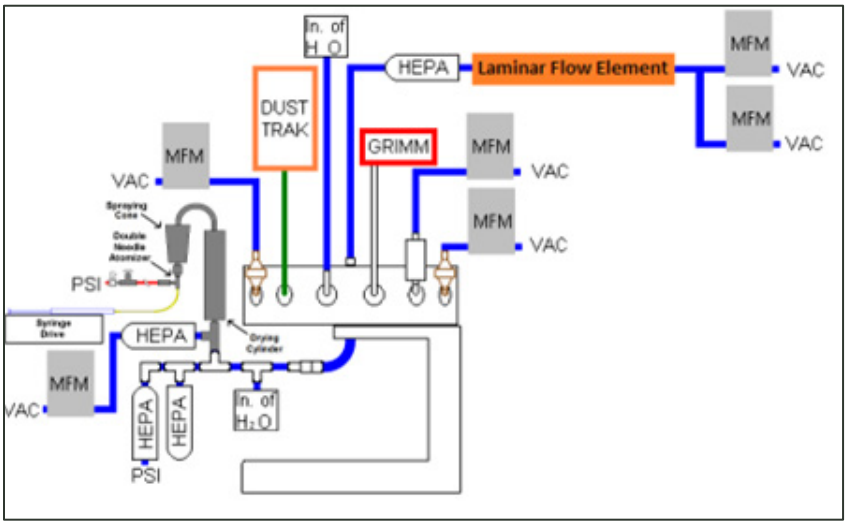

Figure 4. Nose-cone aerosol system.

The Gilibrator calibrator was unplugged and attached to one of the three vacuum lines in the hood (labeled 1–3). The Gilibrator calibrator was primed. At least three Gilibrator measurements were taken, and the average was used as the flow rate. The flow was approximately 1 L/min, ±50 mL. This measuring and averaging process was repeated to determine the flow rate for the other two lines. The cascade impactor and filters were attached to empty ports on the nose-cone setup in opposite, counter-balanced arrangements. The DustTrak

monitor and syringe drive were turned on to a predetermined flow rate. The flow rate varied, depending on the aerosol profile being determined. For experiments in which the apparatus was evaluated for aerosol settling, the system had to be shut down to prevent any airflows. When the system was turned off, the hood vacuum, air valve to DNA, DustTrak monitor, syringe drive, and vacuum pump were all turned off.

2.3 Chamber Aerosol System

All work conducted with the aerosol system was performed under standard operating procedure RNB-323[6] while all equipment and materials were at least 20 cm inside the cell culture hood. The mass flow controller was adjusted to the correct flow rate and maintained in the control position. The exhaust, bleed-off line, and bypass circuit mass flow meter (MFM) were set to the Read position. The vacuum pumps and system were then turned on. The bleed-off line and the associated vacuum pump were only used if needed to remove aerosol and thereby decrease concentrations. The aerosol monitor was turned on to monitor the aerosol generation. Figure 5 shows the aerosol chamber system configuration.

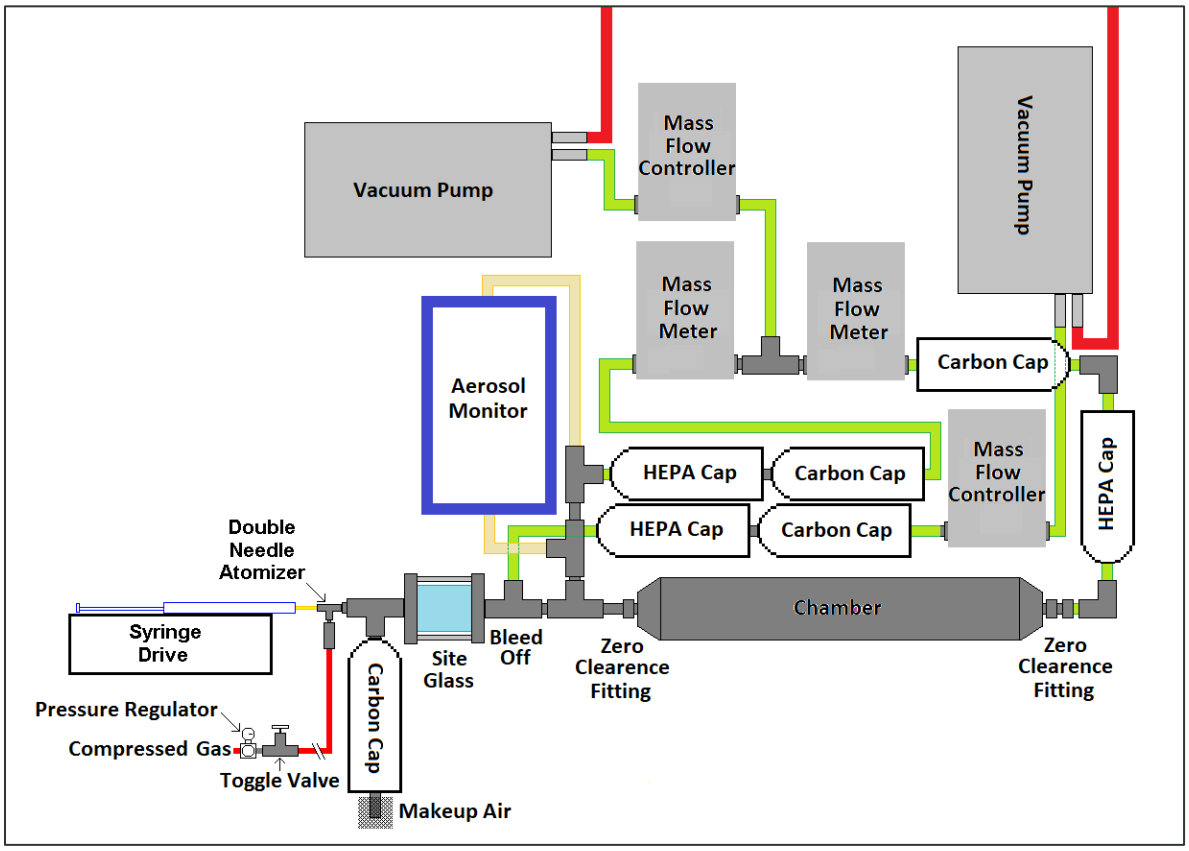

Figure 5. Aerosol chamber system configuration. Cap, capsule.

When the aerosol chamber was set up for the organ chips, the cradles containing the chips were placed into the guide pin slots and locked into the chamber docking port. With the pins completely to the rear of the slots, once flipped up, the OOC forms a compression seal with the labyrinth seal on the chamber. This was repeated for all the chip slots. For any location without a viable chip, a substitute PDMS chip was used without microfluidics; this nonfunctional chip was termed a PDMS slug. Next, the chamber containing the chips was attached to the aerosol generation system through inlet zero-clearance O-ring fittings. These were sealed in place by tightening the nut on the ½ in. NPT (National Pipe Thread) threading.

The Hamilton syringe was loaded with liquid in the same manner as described for the nose-cone-only aerosol system. Once the syringe was loaded and placed into the syringe drive with the syringe drive adjusted to the correct diameter of needle used and desired flow rate, the compressed air was turned on. The syringe drive was then started to allow the feed line to prime with the liquid to be aerosolized. The syringe feed rate was adjusted using the bleed-off line to achieve the desired reading on the aerosol monitor (aerosol concentration). Once the aerosol concentration was adjusted and the bypass line was primed, the chamber MFM was switched to Read and the bypass MFM was closed. Ten times the volume of the aerosol chamber was passed through the chamber before the system was stopped and the aerosol was allowed to settle on the chips. When the system was stopped, everything was turned off, including the vacuum pumps, syringe drive (the block was pulled back from the plunger), compressed air, etc. This was to prevent any air flow in the chamber and allow the aerosol particles to settle on the chips using a predetermined settling time.

Next, the aerosol chamber system was cleared of the airborne aerosol and OOCs were removed. The exhaust and bypass MFMs were set to open, and the corresponding vacuum pump and compressed air were turned on. The aerosol monitor was used to identify the aerosol remaining in the system, until the reading was zero. The bypass MFM was closed, and the chamber MFM was opened to allow a minimum of 20 times the volume of the aerosol chamber to be passed through the chamber. The chamber was disengaged and the OOCs were retrieved. After aerosol administration, the system was shut down, and the DNA was rinsed.

2.4 Construction of Open-Top Lung Chips

The silicone polymer used for construction of the open-top lung chips was PDMS. This polymer is ideal for OOC technology owing to the biocompatible nature of the material, as it allows gas exchange. It is optically clear, elastic, deformable, and inexpensive. Once the molds were developed, the next step of the device process was to fill the molds with PDMS. The final mixture included a 10:1 ratio of PDMS base to PDMS elastomer. After the base–elastomer mixture was weighed, the material was mixed with a tongue depressor in a mixing container. The container was placed in a desiccator attached to a vacuum line for ~20 min or until the air bubbles stopped forming. The desiccated mixture was poured into the device mold, and any excess was scrapped off the top with a flat-edge ruler. A toothpick was used to remove any air bubbles that formed in the process. The PDMS-filled molds were placed in an oven at 150 °F for 5 h to allow the material to fully polymerize and harden. Once the PDMS was fully polymerized, a scalpel was used to cut the pieces out of the mold.

A plasma gun was used to adhere both sides of the chip together, and in the future, a membrane will also be included between both sides. Plasma treatment is commonly a part of developing microfluidic devices made of PDMS because of the surface activation process (Figure 6).[2] During treatment, the methyl groups in silicon in the untreated PDMS are replaced with hydroxyl groups. This allows a fast nucleophile–electrophile reaction that forms covalent bonds between the two previously separated PDMS pieces.

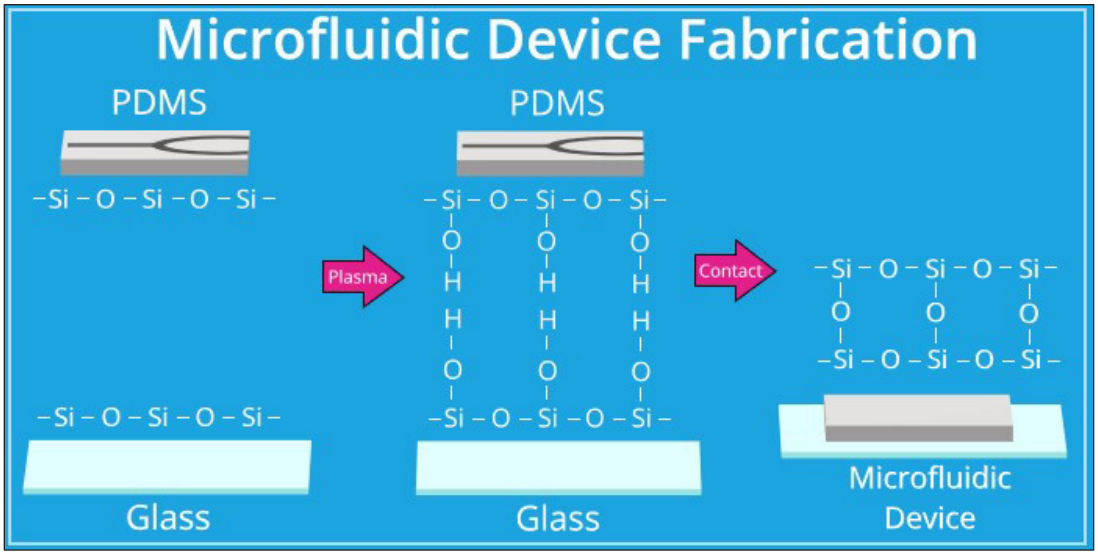

Figure 6. Chemical process of surface activation through oxygen-plasma treatment.[2]

2.5 Quantification of Methacholine

All methacholine samples were analyzed using a 1200 series liquid chromatography system coupled to a 6490 triple-quadrupole tandem mass spectrometry system (LC/MS–MS; Agilent Technologies). Injections (1 µL) with a 5 s methanol needle wash were made with a constant flow of 0.5 mL/min through an Acquity ethylene-bridged hybrid (BEH) hydrophilic interaction chromatography (HILIC; 2.1 × 50 mm, 1.7 µm) analytical ultra-performance liquid chromatography column (Waters Corporation; Milford, MA). The mobile phase was a gradient separation beginning with 95% organic phase (0.1% formic acid in acetonitrile) and 5% aqueous phase (0.1% formic acid in deionized water) with a 0.2 min hold time followed by a linear gradient to 100% aqueous phase at 0.7 min and returning to starting conditions at the 1.0 min mark with a 0.5 min post-run equilibration time. The methacholine target compound and acetylcholine internal standard peaks eluted at 0.76 and 0.77 min, respectively.

The LC/MS–MS system was equipped with an electrospray ionization source with jet stream under positive polarity. The gas temperature was 200 °C at a flow rate of 15 L/min, the nebulizer pressure was 20 psi, the sheath gas temperature was 250 °C at a flow rate of 9 L/min, the capillary voltage was 1300 V, and the charging voltage was 400 V. The fragmentor voltage was 380 V, the MS1 resolution was set to Wide, the MS2 resolution was set to Unit, and the

dwell time for all transitions set to 125 ms. The MS–MS system was operated in multiple-reaction monitoring (MRM) mode. For methacholine, the MRM program monitored one transition for quantitation (mass-to-charge ratio [*m/z*] of 160.1 > 101.1, collision energy of 9 V, and cell accelerator voltage of 7 V) and one for confirmation (*m/z* 160.1 > 42.9, collision energy of 21 V, and cell accelerator voltage of 7 V). For the acetylcholine internal standard, the MRM program monitored one transition for quantitation (*m/z* 146.1 > 87, collision energy of 13 V, and cell accelerator voltage of 7 V) and one for confirmation (*m/z* 146.1 > 43, collision energy of 37 V, and cell accelerator voltage of 7 V).

Calibration curves were created using a weighted ($1/x$) linear regression across a concentration range of 5–1000 ng/mL methacholine, and an acetylcholine internal standard concentration of 200 ng/mL; the resulting correlation coefficient was ≥0.99. During each analytical sequence, a blank internal standard solvent spike and a methacholine quality-control solvent spike were analyzed to confirm that the spiking standard solutions were of the correct concentration and the LC/MS–MS was operating properly.

Samples of the initial ethanol extraction mixture were analyzed by either adding 2 µL of 10 µg/mL acetylcholine internal standard to 100 µL of sample or by diluting 10 µL aliquots of the ethanol extract into 100 µL of ethanol and adding 2 µL of 10 µg/mL acetylcholine internal standard for a sample dilution factor of 10. The results were calculated using the appropriate dilution factor and were reported as the sample solution concentration as received.

3. RESULTS

3.1 Nose-Cone Lower Respiratory Adapter

Two different 3D-printed interfaces were created for the nose-cone aerosol system and the Emulate chip design. One was designed to draw the aerosol over the top of the chip and then stop the aerosol flow over the chip; any sedimentation or diffusion that occurred would account for deposition onto the epithelial cells within the OOC. This model is represented in Figure 7. The sedimentation model represents the deep lung or alveolar region of the lungs, where sedimentation and Brownian motion are the primary methods for aerosol deposition. Modifications were made to adjust the headspace above the open-top organ chips to optimize the amount of material deposited onto the epithelial cells. Higher headspace led to higher deposition of aerosolized material, while lower headspace led to lower deposition of aerosolized material.

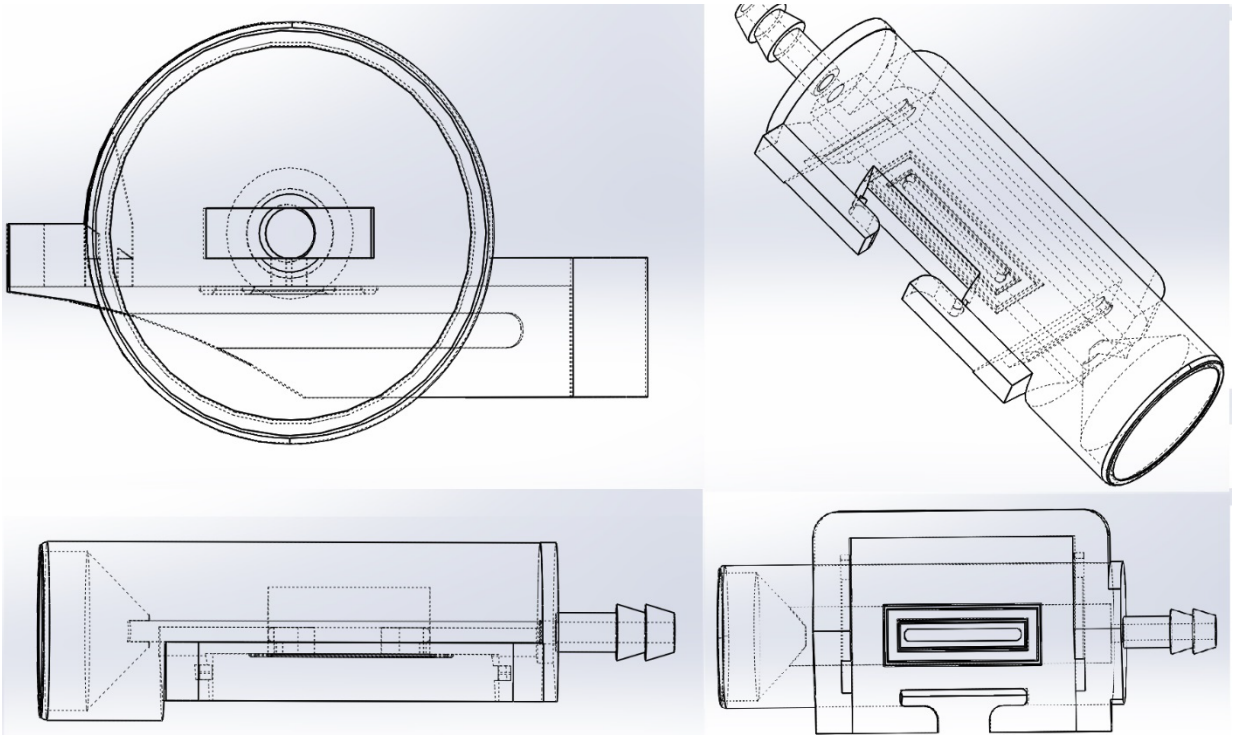

Figure 7. Nose-cone lower respiratory OOC adaptor. Clockwise, from top left: front view, perspective view; bottom view, and lateral view.

3.2 Nose-Cone Upper Respiratory Adapter

The other 3D-printed interface for OOC technology with the nose-cone aerosol generating system was designed for deposition to occur via impaction. This models the upper respiratory tract, where impaction of aerosol particles is the primary method for deposition. This relied on a bilateral vacuum to pull the aerosol uniformly over the epithelial cells in the OOC (Figure 8).

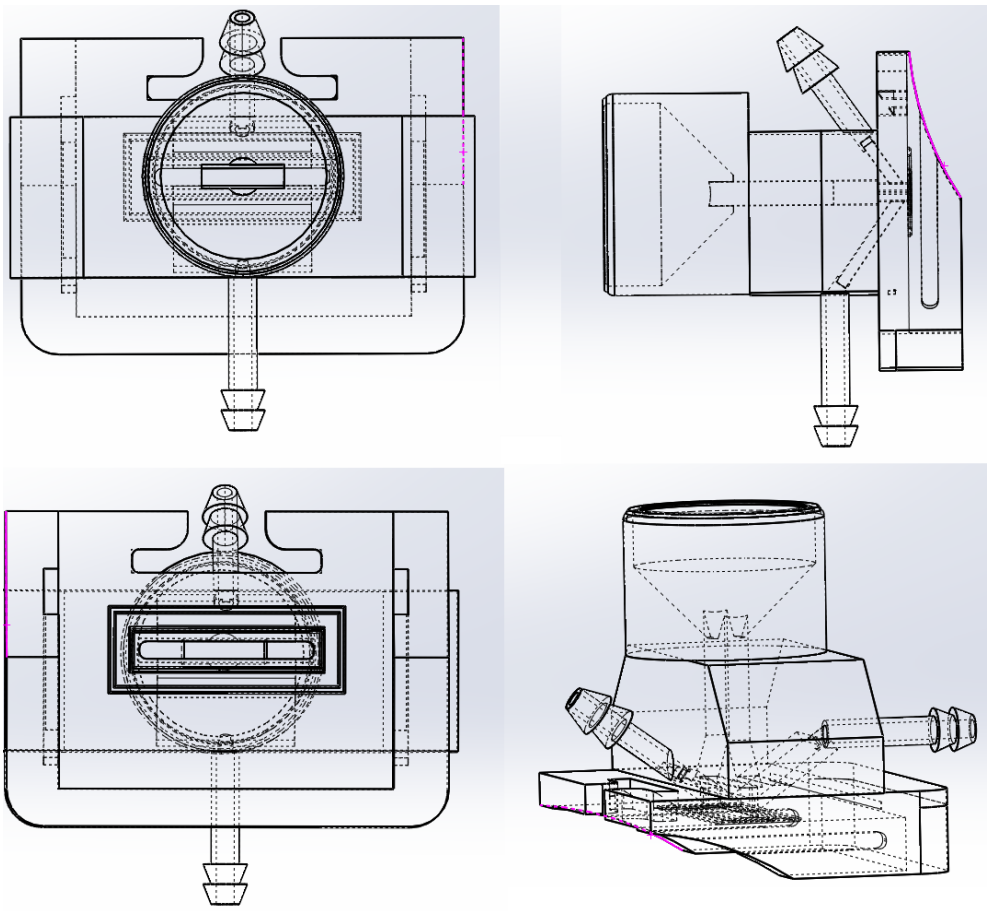

Figure 8. Nose-cone upper respiratory OOC adaptor. Clockwise, from top left: front view, lateral view, perspective view, and bottom view.

Both adaptors allowed for deposition to occur onto OOCs at physiologically relevant concentrations. Additionally, the adaptors were completely sealed to prevent agent contamination. The PDMS in the chips forms a tight seal with the exposed window for the 3D-printed adaptors. The aerosol adaptors have labyrinth seals surrounding the window to expose the OOC and create a strong seal. All the 3D-printed aerosol adaptors are disposable, enabling easy decontamination after use.

3.3 Characterization of Nose-Cone OOC Aerosol Adaptors

The method for the nose-cone aerosol system was performed using 10 mg/mL methacholine in 200 proof ethanol as solvent at an injection rate of 15 µL/min and a flow rate of 950–1000 mL/min. For each run, a cascade impactor was used to determine the aerosol profile.

The MMAD was calculated using a two-point interpolation of the NORMSINV analysis. This analysis is determined from the zero standard deviation (SD) intercept of the two-point line that spans the zero SD point. The geometric standard deviation (GSD) for the two-point interpolation of the NORMSINV analysis is determined from the slope of the two

points that span the zero SD point ±1 SD on either side of the median.[3–5] The results for the cascade impactor are shown in Tables 1 and 2 and Figures 9 and 10. The MMAD was calculated to be 1.69 µm, which is the ideal range for deep lung exposure to aerosol particles. These particles will also deposit in the upper airways; however, the primary objective of this aerosol generation was to reach the deep lungs.

Table 1. Cascade Impactor Stage Results

Stage	Cutoff Diameter (mm)	Response*	Cumulative†
1	4.75	0.283286119	100
2	3.1	12.46458924	99.71671388
3	2.16	21.6713881	87.25212465
4	1.68	14.06987724	65.58073654
5	1.1	26.01510859	51.5108593
6	0.74	9.39565628	25.49575071
7	0.34	12.41737488	16.10009443
8	0	NA	3.682719547

*Percentage of total amount of aerosolized compound that was contained on that plate of the cascade impactor.
†Amount of total aerosol that interacted with that particular plate of the cascade impactor (starting at 100%, then steadily decreasing as aerosol was trapped at plates).
NA, not applicable.

Table 2. Two-Point Interpolation of NORMSINV Data

Parameter	Two-Point Interpolation of NORMSINV Data
MMAD	1.690 µm
GSD	1.958
Total response	96.31
Data points	2
Slope	0.29172 µm
Intercept	0.22782 µm

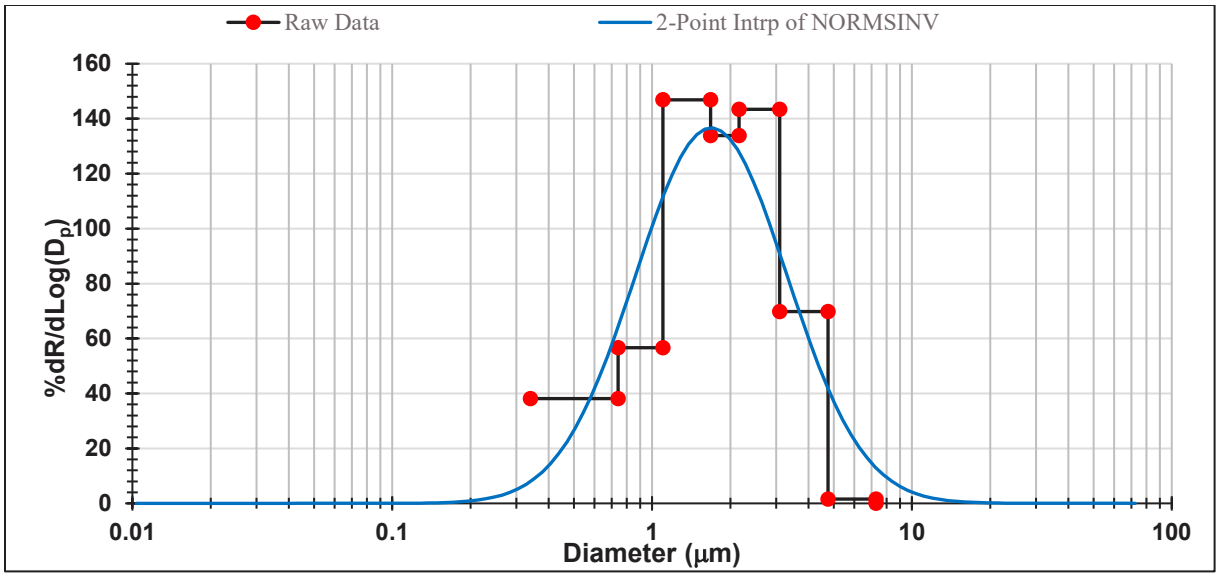

Figure 9. Calculation of MMAD using two-point interpolation of NORMSINV data with the fractions of each stage of the cascade impactor, relative to the total mass of aerosolized agent in the cascade impactor.

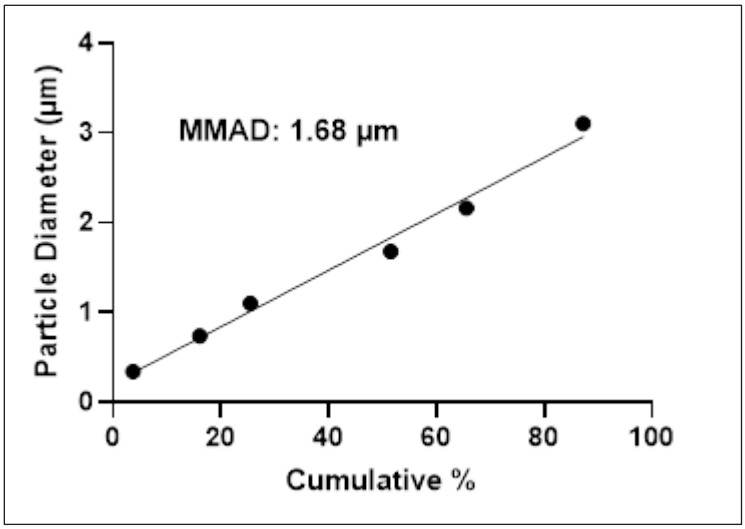

Figure 10. Log probability graph: MMAD using cascade impactor.

Deposition was confirmed on both the upper and lower respiratory nose-cone OOC adaptors, Figure 11. The deposition was measured following 10 min of aerosol flow through at the rates described in the first paragraph of this section.

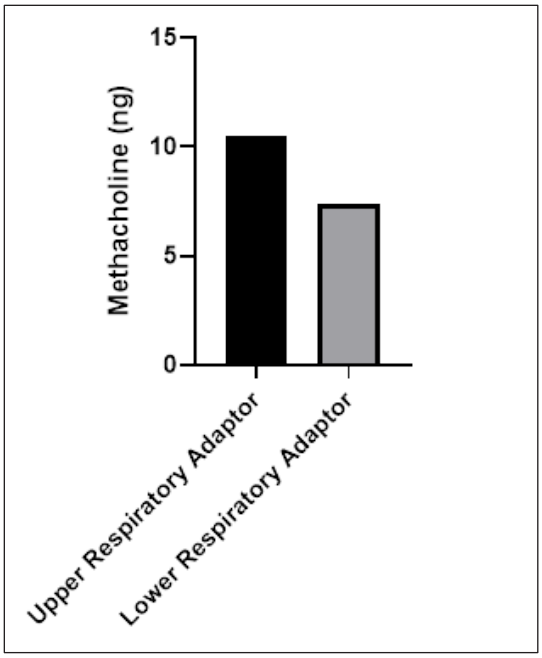

Figure 11. Methacholine deposition in nose-cone aerosol system.

3.4 Open-Top Chip Fabrication

The Emulate chips are a completely closed system, and modification was necessary to allow for aerosol deposition to occur with the designed adaptors. This required an open-top OOC design. SLA was the method used for 3D printing. The Saturn 4K Mono SLA instrument (Elegoo; Shenzhen, China) has a 60 µm feature resolution limit. This meets the requirements for two of the three master molds; however, the membrane master mold requires features of 5–7 µm. Microscale SLA was used to eliminate the photoetching process yet still permit the low-micron features necessary in the membrane master mold. This final low-micron master mold was used with the microArch S230 micro-SLA printer (BMF). The membrane master mold was manufactured at the micro scale with a feature resolution limit of 2 µm. Once the molds were made, degassed PDMS combined with hardening agent was poured into the 3D-printed molds and cast. This required baking the PDMS overnight at 140 °F.

The bottom half of the master mold contained the lower channel and two parallel vacuum channels (Figure 4). The lower channel with cells was 800 µm in width and 17 mm in length. The vacuum channels were 400 µm in width and 17 mm in length. The PDMS chip was 38 × 12.7 × 4 mm. However, the depth of the chip was modified to best accommodate aerosol deposition onto epithelial cells. Initially, the channels were placed in the middle of the chip (2 mm depth); however, optimization revealed that a 1 mm depth for the open-top upper channel was best for aerosol deposition to occur. Therefore, the lower channel molds were 3 mm in depth. The molds for both the upper and lower chips were designed to accommodate as few as one chip (Figure 12) to as many as 10 chips.

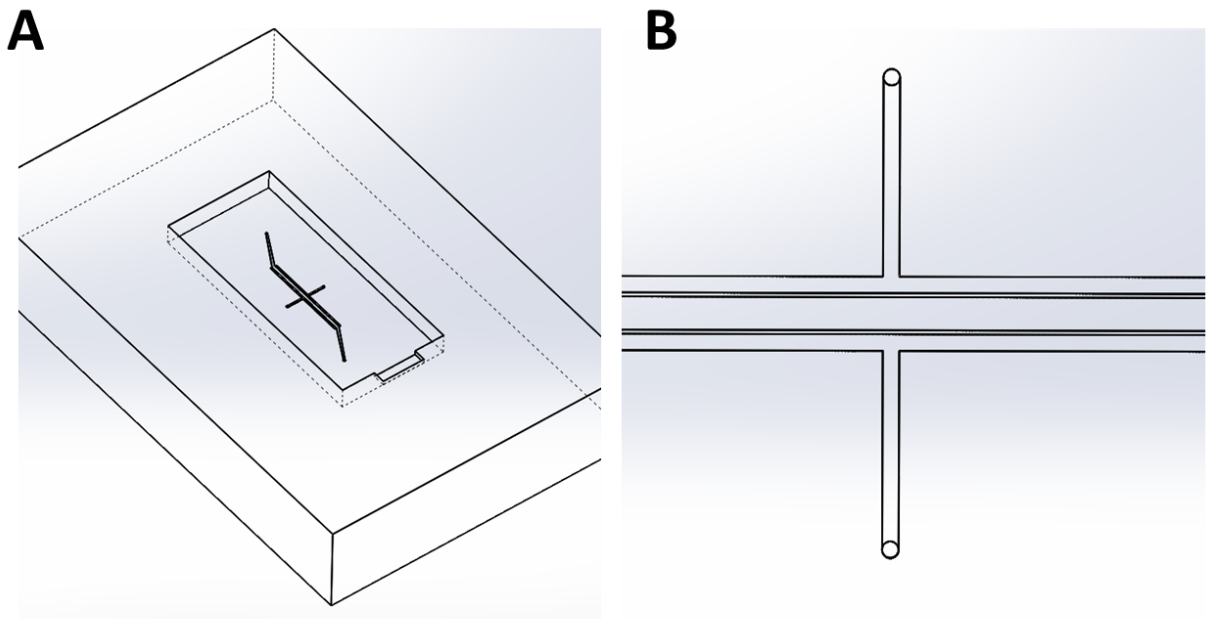

Figure 12. Lower half of open-top chip mold. A: lower half of chip mold. B: channels in chip.

The upper half of the mold was modified to allow an open-top chip design. This enables aerosols to be deposited on the epithelial cells of the chips. The optimal depth for the upper piece of the chip was determined to be 1 mm (Figure 13).

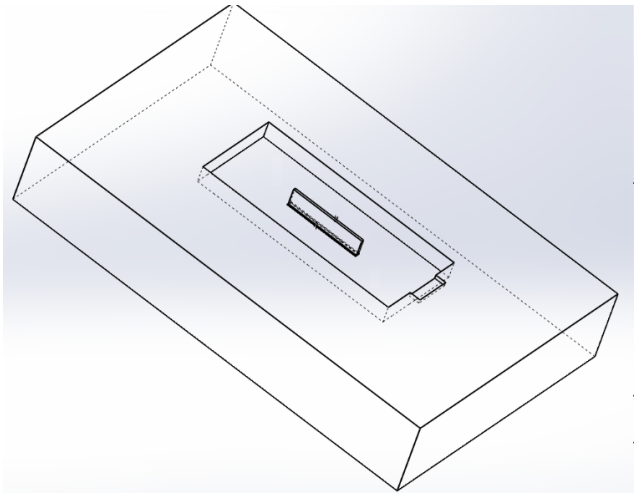

Figure 13. Top half of open-top chip mold.

A lid for the open-top chip was designed to maintain our ability to place the chips under perfusion. This required a completely closed system. The lid mold was designed using the SLA printer and cast using PDMS (Figure 14). As an alternative, a thin coat of PDMS (approximately 50–100 µm) was spun and placed over the exposed channel of the chip to allow perfusion.

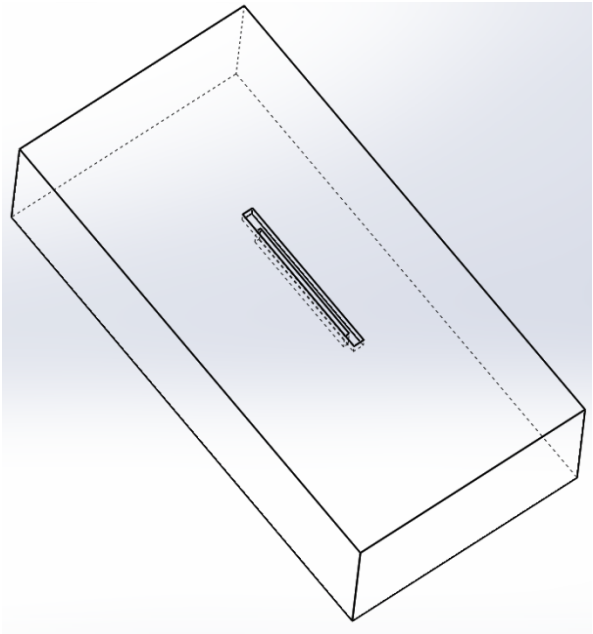

Figure 14. Open-top chip lid.

3.5 Chip Membrane Molding

A membrane was molded to fit in between the top and bottom channels. The membrane requires a mold with posts that are <10 µm in diameter, and 7 µm was determined to be preferable. This required that a part be printed using the microArch S230 micro SLA printer with a 2 µm resolution limit. The posts were printed at 10 µm spaced uniformly 25 µm apart (center-to-center spacing), as shown in Figure 15. The membrane was cast 50 µm thick. A spin coater was used to apply uncured PDMS to the membrane mold. When a 50 µm thickness was achieved, the PDMS membrane was removed from the mold.

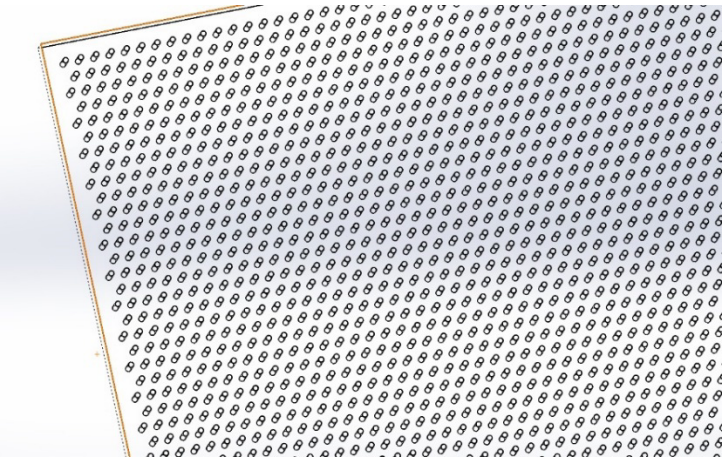

Figure 15. Membrane for open-top organ chip.

Once the 3D-printed master molds were complete, chip components were cast using PDMS as the biocompatible material. All three pieces of the chips were plasma treated to fuse into a finished organ chip. Each plasma-activated PDMS section of the chip was stacked; dowel pins in the molds allowed for alignment of the channels. This research required the development of a novel open-top lung chip design with an adaptable aerosol and vapor system that seamlessly interfaces with the lung chip platforms.

3.6 Plasma Treatment for Construction of Open-Top Chip

To identify which time point would be optimal for our device specifically, multiple time points for plasma treatment were tested in replicates of three. After the selected time of plasma treatment, the pieces were adhered and placed in the oven at 150 °F under a uniform weight. After 24 h, the pieces were evaluated for adherence. A Likert scale was used to quantify how well the pieces were stuck together (1, easy to pull apart; 3, some resistance to being pulled apart; and 5, very difficult to pull apart). The results are listed in Table 3. The most optimal time was discovered to be 90 s of plasma treatment.

Table 3. Results from Plasma Treatment Testing*

Time of Plasma Treatment (s)	Average Rating (scale, 1–5)
15	3
30	4
45	4
60	4.5
90	5
120	3

*n = 3 ratings.

Because Emulate did not provide exact dimensions for the top and bottom layers, one of the tasks was to select the ideal thicknesses for these layers. Three different parameters were tested (Table 4), each with a total thickness of 6 mm to mimic the Emulate chip.

Table 4. Optimizing Chip Layer Thickness

Top Layer (mm)	Bottom Layer (mm)	Total Thickness (mm)
1	5	6
2	4	6
3	3	6

Based on the plasma treatment protocol mentioned above, each parameter was tested for adherence. The Likert scale was used to measure the adherence, and all three parameters performed well (rating of 5). The 1 mm top and 5 mm bottom layers were chosen to better replicate the Emulate chip. The in-house chip was tested for compatibility with the Emulate system.

3.7 Development of Open-Top Chip Aerosol Chambers

The aerosol system from Figure 16 was designed specifically for aerosol deposition onto OOC technology. For this system, we designed chambers that can accommodate multiple chips simultaneously. The chamber in Figure 16 was designed to interface with the open-top Emulate chips, and the chamber in Figure 17 was designed to interface with TissUse chips (TissUse GmbH; Berlin, Germany).

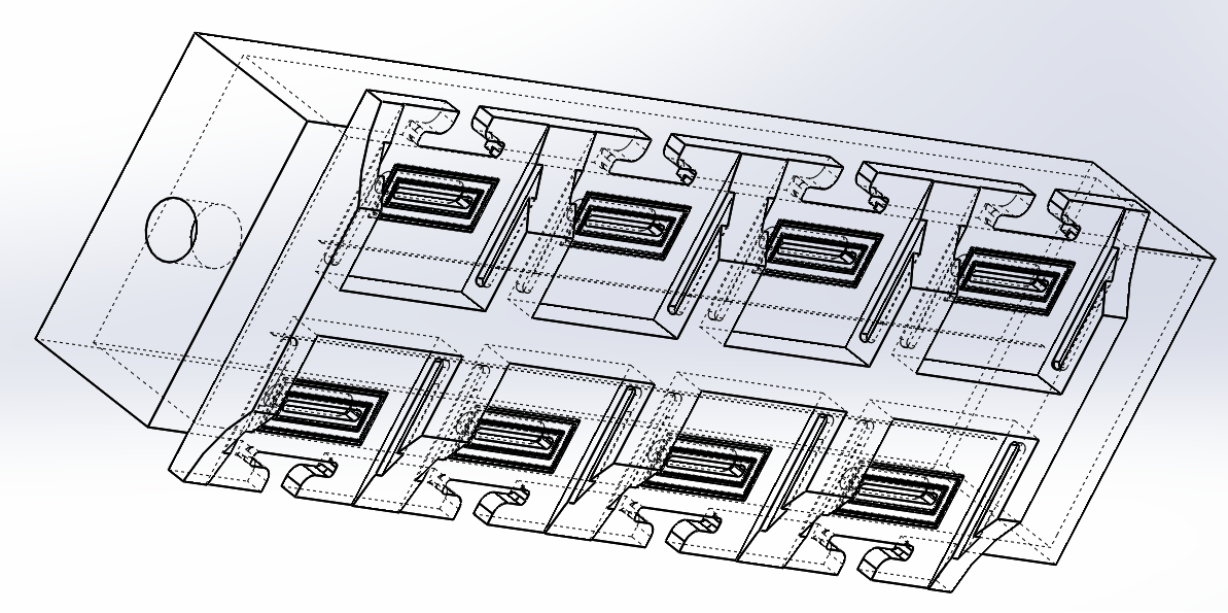

Figure 16. Open-top chip aerosol chamber.

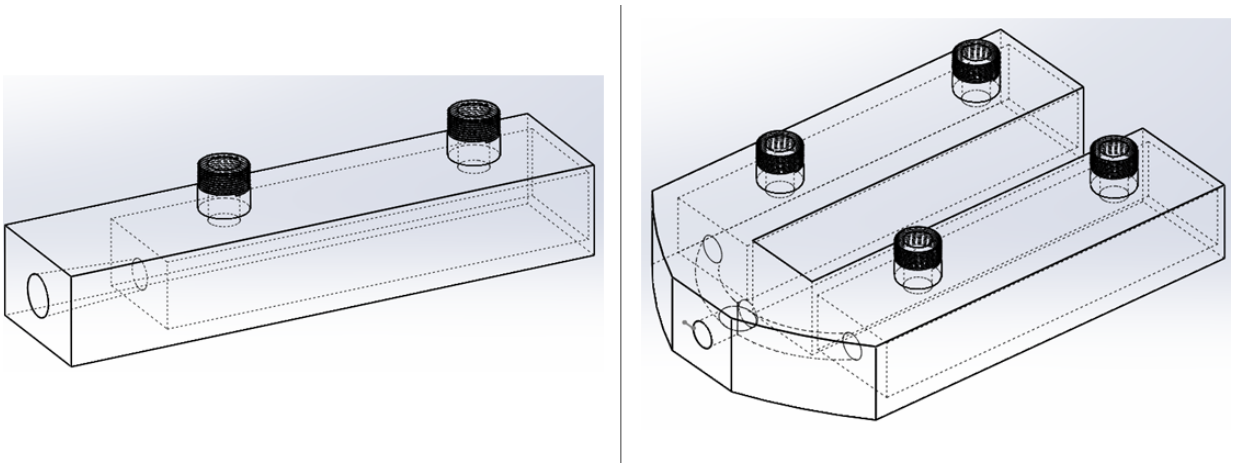

Figure 17. Two TissUse aerosol chambers. (Left) chamber can accommodate two OOCs; (right) chamber can accommodate four OOCs.

The chambers for both the TissUse and the modified Emulate chips were designed to prevent any aerosol exposure outside of the epithelial cells within the chambers. This was a requirement, given the nature of the chemical and biological warfare agents that would be aerosolized. The Emulate system maintained pressure in the aerosol system via labyrinth seals, and the TissUse system maintained pressure via threaded attachments with O-rings.

3.8 Characterization of Open-Top OOC Aerosol Chambers

Two different chambers were chosen to demonstrate deposition on the OOC for the TissUse system. One chamber had a ceiling height (inside the chamber) of 1.11 in., and the other had a higher ceiling height of 3.33 in. Figure 17 shows the chamber design. A 10 mg/mL solution of methacholine chloride in 200 proof ethanol was injected into the double-needle atomizer at a rate of 20 µL/min. The flow rate through the chamber was 30 L/min, and the bleed-off line was not opened. The chamber was filled with aerosol to 10-fold the volume of the chamber (30 s fill time) using the procedure outlined in Section 2.3. Once the chamber was filled and the flow eliminated, the aerosol was allowed to deposit on the OOCs for 10 and 20 min in the small and large chambers, respectively.

The settling velocity (V_{ts}) was calculated using

$$V_{ts} = \rho d D^{2gC/18\eta} \quad (1)$$

and

$$V_{ts} = 0.003 \rho d D^2 \quad (2)$$

where ρd is particle density (in g/cm^3), D is the diameter of the spherical solid (in µm); g is the settling velocity of the aerosol (in m/s^2); C is the Cunningham slip correction factor; and η is the viscosity of fluid (in Pa-s) at room temperature and standard atmospheric pressure. The settling times for the large and small chambers were 15 and 6.8 min, respectively. The deposition time exceeded both calculated settling velocity times to ensure that full deposition occurred. The

theoretical deposition was calculated using the dimensions of both chambers, the concentration of aerosol inside the chamber, and the volume of aerosolized material in the headspace above the OOC ports. The results from the methacholine deposition (using significantly higher experimental deposition than was calculated theoretically) are shown in Figure 18. The discrepancy in the deposition likely occurred when filling the chamber with aerosol. At this stage, aerosol will still deposit on the OOC. This can be mitigated in future runs by limiting the fill step to 5 and 15 s for the small and large chambers, respectively. These values were calculated given the flow rates used for the deposition experiment. Although the magnitude was off by a factor of 10, the deposition ratio was consistent between the small and large chambers. This test confirmed that we were successful in depositing aerosolized material on the OOC, and the chamber design can control the deposition that occurs on the OOC.

The aerosol was deposited on Parafilm laboratory film (Amcor; Zurich, Switzerland) wrapped around the end of the aerosol chamber ports. The Parafilm was then removed and washed in 200 proof ethanol inside a 1.5 mL microcentrifuge tube. The samples were processed in triplicate and analyzed using HPLC/MS–MS.

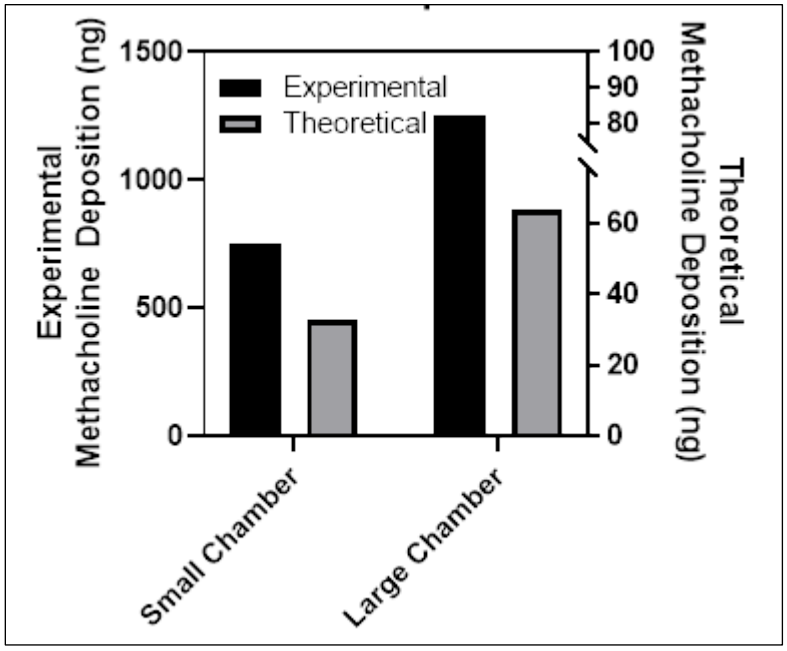

Figure 18. Aerosol deposition in the small and large chambers.

3.9 Development of Vapor Delivery Chambers

In addition to the aerosol exposure systems, both the TissUse and the Emulate systems were modified for exposure to vapors. The 3D-printed lid that was modified for vapor exposure to the Emulate and TissUse chips is shown in Figure 19. The vapor system did not necessitate modification of the Emulate chips because the vapor does not have the same limitations as the aerosol, where deposition is modified by sharp turns and microfluidics. The lid for the Emulate chip and the container (box) for the agent were filled to the top with a silicon

polymer such as PDMS to enable a tight seal when compressed. The lid that came with the Emulate pod system was replaced with this vapor lid, and vapor was fed into the appropriate channel. The inlet ports for the lid interfaced with the microfluidics for the chips. The ends of the ports were also coated in silicon polymer, as this malleable material can create a tight seal.

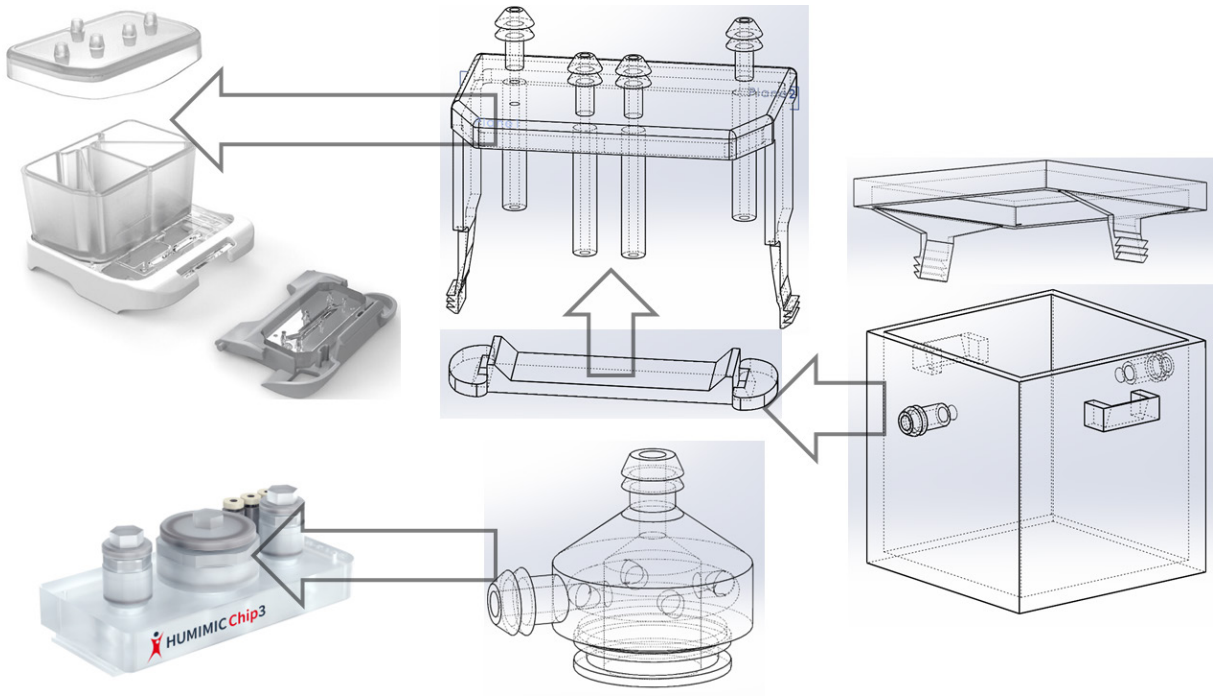

Figure 19. Emulate (top) and TissUse (bottom) vapor systems. The 3D-printed box houses the agent intended for vapor deposition. Vapor travels from the box to the inlet ports of the Emulate pod system or directly to the tissue in the TissUse system.

4. CONCLUSION

This study successfully combined two distinct OOC technologies with aerosol technology to create a physiologically relevant human respiratory exposure model. Aerosol deposition on the OOCs was accomplished via two different aerosol systems: the nose-cone aerosol system and the aerosol OOC system specifically designed to deposit aerosols onto OOC technologies. Both systems used similar aerosol generation technology (DNA) and were confirmed to deposit aerosolized material on OOCs at physiological concentrations and droplet sizes representative of those for a human lung. The aerosol profiles generated matched the physiological range of the aerosol droplet size for the lower respiratory system at an MMAD of 1.69 µm. The quantity of deposited aerosol was representative of the proportionate mass of lung tissue exposed to an aerosolized agent (1–100 ng quantities).

During the project, we successfully redesigned two existing OOC technologies (Emulate and TissUse) to make them amenable to aerosol deposition. Additionally, the technology was designed to accommodate the rigorous safety requirements for working with

chemical and biological warfare agents. The additively manufactured aerosol adaptors are single use and can be destroyed after exposure. The 3D printing systems include customizable time- and cost-effective parts, which allowed us to apply this technology to manufacture novel aerosol delivery systems for lung tissue exposures in vitro. By producing an aerosol delivery system amenable to a lung chip, we filled a gap in our current technology by enhancing and expanding our repertoire of testing available to lung microenvironments. We designed, generated, and evaluated novel open-top lung chips that will be used downstream to facilitate the unique needs of the U.S. Army's aerosol toxicological agent assessments.

LITERATURE CITED

1. McCaskey, D.A. Coaxial Needle Atomizing System. US 9,016,671 B1, 2015.

2. PDMS Bonding (Microfluidics). Harrick Plasma: Ithaca, NY. https://harrickplasma.com/pdms-bonding/ (accessed 13 May 2024).

3. Hinds, W.C. *Aerosol Technology, Properties, Behavior, and Measurement of Airborne Particles,* 2nd ed.; John Wiley & Sons: Hoboken, NJ, 1995.

4. *Anaesthetic and Respiratory Equipment—Nebulizing Systems and Components*; ISO 27427:2013; International Organization for Standardization: Geneva Switzerland, 2013. https://www.iso.org/standard/59482.html (accessed 9 April 2024).

5. Sánchez Jiménez, A.; Galea, K.S.; Aitken, R.J. *Guidance for Collection of Relevant Particle Size Distribution Data of Workplace Aerosols—Cascade Impactor Measurements*; Report TM/09/04; Institute of Occupational Medicine (IOM-World): Edinburgh, U.K., June 2011.

6. Fudge, D.; Dhummakupt, E. *Aerosol Testing Using a Containment Chamber*; RNB-323; U.S. Army Combat Capabilities Development Command Chemical Biological Center: Aberdeen Proving Ground, MD, 2022.

Blank

ACRONYMS AND ABBREVIATIONS

BMF	Boston Micro Fabrication
DEVCOM CBC	U.S. Army Combat Capabilities and Development Command Chemical Biological Center
DNA	double-needle atomizer
GSD	geometric standard deviation
HPLC	high-performance liquid chromatography
LC	liquid chromatography
MFM	mass flow meter
MMAD	mass median aerodynamic diameter
MPS	microphysiological system
MRM	multiple reaction monitoring
MS	mass spectrometry
m/z	mass-to-charge ratio
NPT	National Pipe Thread
OOC	organ-on-a-chip
PDMS	polydimethylsiloxane
SD	standard deviation
SLA	stereolithography

Blank

DISTRIBUTION LIST

The following individuals and organizations were provided with one electronic version of this report:

U.S. Army Combat Capabilities Development Command Chemical Biological Center (DEVCOM CBC)
Molecular Toxicology Branch
FCDD-CBR-TM
ATTN: Fudge, D.
Lee, P.
Evans, R.
Goralski, T.
Ellis, C.
Ruprecht, B.

DEVCOM CBC Technical Library
FCDD-CBR-L
ATTN: Foppiano, S.
Stein, J.

Defense Technical Information Center
ATTN: DTIC OA

U.S. ARMY

U.S. ARMY COMBAT CAPABILITIES DEVELOPMENT COMMAND
CHEMICAL BIOLOGICAL CENTER